# PLOS ONE

# A novel bioassay to detect Nociceptin/ Orphanin FQ release from single human polymorphonuclear cells

M. F. Bird[1‡], C. P. Hebbes[1‡], S. W. M. Scott[1], J. Willets[2], J. P. Thompson[1], D. G. Lambert[1]*

1 Departments of Cardiovascular Sciences, University of Leicester, Anaesthesia, Critical Care and Pain Management, Leicester, United Kingdom, 2 Molecular and Cell Biology, University of Leicester, Anaesthesia, Critical Care and Pain Management, Leicester United Kingdom

‡ MFB and CPH are joint first authors on this work.
* dgl3@le.ac.uk

## Abstract

Nociceptin/Orphanin FQ (N/OFQ) is the endogenous opioid agonist for the N/OFQ receptor or NOP. This receptor system is involved in pain processing but also has a role in immune regulation. Indeed, polymorphonuclear cells (PMNs) express mRNA for N/OFQ precursor and are a potential source for circulating N/OFQ. Current measurements are based on ELISA and RIA techniques. In this study we have designed a bioassay to measure N/OFQ release from single PMNs. Chinese Hamster Ovary (CHO) cells transfected with the human (h) NOP receptor and $Ga_{iq5}$ chimera force receptor coupling in biosensor cells to increase intracellular $Ca^{2+}$; this can be measured with FLUO-4 dye. If isolated PMNs from healthy human volunteers are layered next to $CHO_{hNOPGaiq5}$ biosensor cells then stimulated with the chemoattractant N-formyl-methionyl-leucyl-phenylalanine (fMLP) we hypothesise that released N/OFQ will activate the biosensor. PMNs also release ATP and CHO cells express purinergic receptors coupled to elevated $Ca^{2+}$. In a system where these receptors (P2Y1, P2Y2 and P2X7) are blocked with high concentrations of PPADS and oATP, PMN stimulation with fMLP increases $Ca^{2+}$ in PMNs then shortly afterwards the biosensor cells. Our data therfore reports detection of single cell N/OFQ release from immune cells. This was absent when cells were preincubated with the selective NOP antagonist; SB-612111. Collectively this is the first description of single cell N/OFQ release. We will deploy this assay with further purified individual cell types and use this to further study the role of the N/OFQ-NOP system in disease; in particular sepsis where there is strong evidence for increased levels of N/OFQ worsening outcome.

## Introduction

The Nociceptin opioid receptor (NOP) is the most recently discovered member of the opioid receptor family and is activated by an endogenous peptide agonist Nociceptin/Orphanin FQ (N/OFQ) [1]. Despite sharing a common transduction mechanism with classical opioid

receptors, NOP has little or no affinity for ligands associated with classical naloxone-sensitive opioid receptors (mu:μ:MOP; delta:δ:DOP; kappa:κ:KOP). Importantly, actions at NOP are not sensitive to naloxone [1, 2]. Upon activation, NOP causes activation of the $G_{i/o}$ G-proteins, leading to a decrease in cyclic AMP (cAMP) production, activation of inwardly rectifying potassium channels, closure of calcium channels and activation of the mitogen-activated protein kinase (MAPK) pathway. A significant body of research has focused on the role of NOP in analgesia and pain management. However, NOP is widely distributed in areas of the cardiovascular, immune, and central nervous systems, which suggest it is involved in a broad range of physiological processes [1–3].

NOP, N/OFQ and encoding mRNA have been detected in immune cells of both myeloid and lymphoid lineages [3, 4]. Evidence in patients with asthma, those undergoing surgery under cardiopulmonary bypass, and critically ill patients with sepsis suggest that N/OFQ-NOP may modulate acute inflammatory states, in which polymorphonuclear (PMN or granulocytes) cells play a significant role [3, 5–7]. This assertion is further supported by detection of transcripts encoding NOP and N/OFQ in polymorphonuclear leukocyte cells [6].

N/OFQ is increased in association with arthritis, asthma, sepsis and cardiopulmonary bypass in-vivo [6–8]. In an experimental caecal ligation/puncture model in rats, mortality was increased in animals also treated with exogenous N/OFQ, and mortality was decreased compared with controls in rats treated with the NOP antagonist UFP-101. These data suggest that N/OFQ increases in inflammatory states, and that it may have a modulatory effect on inflammatory processes [5].

However, the underlying source, and target for the observed increase in N/OFQ concentration is unclear. PMNs have a fundamental role in the response to bacterial infection, migrate to sites of inflammation when stimulated, contain NOFQ transcripts and secrete other substances [3]. PMNs are therefore a possible source.

Capturing real-time release of N/OFQ in defined subpopulations of PMNs would improve understanding of its role in the immune response. We describe a method to demonstrate live-cell release of N/OFQ from cells, using mixed PMNs (that produce mRNA for N/OFQ precursor) as a model (**Fig 1**). This biosensor-based approach uses intracellular calcium concentration as a readout via an adapted human NOP receptor with a C-terminally modified $G\alpha_{qi5}$ stably transfected into CHO cells ($CHO_{hNOPg\alpha qi5}$) [9]. If PMN degranulation releases N/OFQ from stores within defined PMN populations this will activate NOP in $CHO_{hNOPg\alpha qi5}$ to increase intracellular calcium concentration ($[Ca^{2+}]_i$). This can be observed in real time using the fluorescent calcium indicator FLUO-4. CHO cells are suited to this application because of the relative ease of transfection, and the existence of well characterised endogenous receptors. However, these cells are known to express purinoceptors [10, 11].

We hypothesised that a proportion of PNMs will release N/OFQ and this could be demonstrated using in $CHO_{hNOPg\alpha qi5}$ biosensor cells and an increase in $[Ca^{2+}]_i$. The aims of this work were to develop and validate this assay system.

## Materials and methods

### Extraction and isolation of PMN cells

Ethical approval was granted from the University of Leicester ethics committee (healthy volunteers). With written informed consent up to 30mls blood was collected from healthy volunteers into the S-Monovette collecting system (Sardstedt, Germany) containing K-EDTA (7.5ml blood per tube, final EDTA concentration 1.6 mg ml$^{-1}$). Our donor pool comprised 16 participants, M:F = 9: 7 and age range 25–55. PMNs were extracted from blood within one hour of sampling by centrifugal separation over an equal volume of Polymorphprep (Axis-Shield,
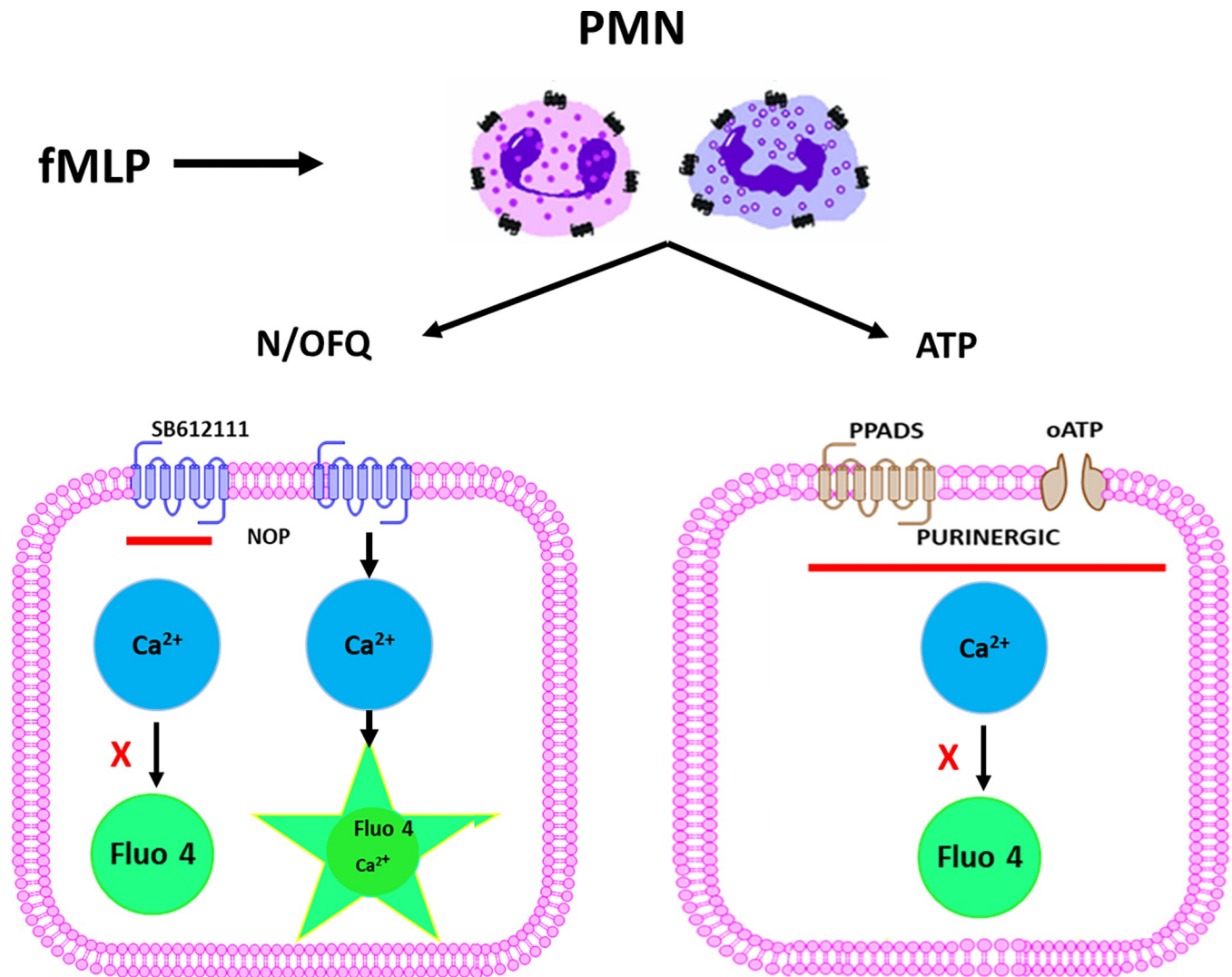
**Fig 1. Schematic of representation of the immune cell bioassay.** If immune cells produce N/OFQ peptide and release it in response to stimulation (with fMLP), released N/OFQ will bind to NOP receptors and chimeric G-protein on the surface of the CHO cell leading to an increase in calcium. This calcium increase can be measured using the fluorescent calcium indicator dye FLUO-4 and should be sensitive to NOP antagonists (SB-612111). CHO cells also express purinergic receptors that increase calcium in response to ATP also potentially released from PNMs; this can be blocked with purinergic antagonists (PPADS and oATP).

Dundee) as described previously [6]. The resulting PMN layer was removed, washed, cleared of erythrocytes by 1:1 dilution with BD PharmaLyse (Becton, Dickinson and Company, Oxford), washed and suspended in Krebs buffer (126 mM NaCl, 2.5 mM KCl, 25 mM NaHCO$_3$, 1.2 mM NaH$_2$PO$_4$, 1.2 mM MgCl$_2$, 2.5 mM CaCl$_2$) for counting and imaging. Extractions were carried out at room temperature, and the resulting cell suspension maintained on ice until use (maximum 4 hours). Viability and yields were quantified by Trypan Blue exclusion and counting using a haemocytometer [12]. For determination of purity samples were further processed on a Becton-Dickinson FACS Aria II counter (BD Biosciences, San Jose, USA) with autoflurescence compensation. Final sample concentration was 1 x 10$^6$ cells ml$^{-1}$ prior to flow cytometry. PMN purity and identity data are presented in **S1 Fig in S1 File**.

## Cell culture

CHO cells transfected with the human NOP receptor and $G\alpha_{iq5}$ chimera ($CHO_{hNOPG\alpha iq5}$) were a gift from Professor G. Calo (University of Ferrara, Italy; originally as a collaboration with Prof T. Costa, Instituto Superiore di Sanita, Rome, Italy). $CHO_{hNOPG\alpha iq5}$ were maintained in Hams 1:1 F12 Nutrient Mix and Dulbecos Minimal Essential Media (DMEM) (Invitrogen), supplemented with 10% Fetal Calf Serum, Penicillin (100 IU ml$^{-1}$), Streptomycin (100 IU ml$^{-1}$) and Amphotericin B (2.5g $10^{-6}$ ml$^{-1}$). All cells were maintained in 5.0% $CO_2$, humidified air, at 37˚C, and routinely subcultured after 2–3 days when $\geq$ 90% confluence had been attained.

## Fluorimetric measurement of changes in $CHO_{hNOPG\alpha iq5}$ $[Ca^{2+}]_i$ in cell populations in response to N/OFQ

Fluorimetry was performed using a Perkin-Elmer LS50B fluorimeter (Beaconsfield, UK) using a standard Fura-2 based method as described [13]. Fluorescent emission was measured at 510 nm, with alternate excitation at 340 nm and 380 nm. Briefly, 2 mls of Fura-2 loaded cell suspension was introduced into a quartz cuvette and stirred using a magnetic stirrer, maintained at 37˚C using a water jacket fed from a thermostatically-controlled water bath in the dark. Fluorescence was measured for 180 seconds prior to the introduction of 50 μl of test compound (40x in-assay concentration), and then until restabilisation of the signal. Following the final sample (per flask), the loading was calibrated to maximal and minimal fluorescence using 0.1% Triton X-100; 50 μl (Sigma Aldrich; Missouri, USA) followed by 4.5 x $10^{-3}$ M EGTA; 150 μl, pH>8 (Sigma Aldrich; Missouri, USA). Test compounds were maintained on ice, and cells were maintained at room temperature, protected from light throughout. Data were analysed using the fluorescence data manager (FLDM) software associated with the LS50B fluorimeter (Perkin-Elmer, Beaconsfield, UK). Raw fluorimetry data were processed using per-batch calibration, and values substituted into the Grynkiewicz equation [14] by FLDM software.

## Confocal measurement of changes in PMN and $CHO_{hNOPG\alpha iq5}$ fluorescence

28mm Number 1 coverslips (Thermo-scientific, UK) were sterilised in absolute ethanol, coated with CellTak™ tissue adhesive (Corning, New York USA) by adsorption, air dried, and stored at <5˚C for a maximum of 7 days. Prepared coverslips were seeded with $CHO_{hNOPG\alpha iq5}$ (2.5–5 x $10^4$ cells per coverslip) and incubated as for cell culture for 18–24 hours before use. When ready for use, seeded coverslips were incubated with 6 x $10^{-6}$ M of the $[Ca^{2+}]_i$ dye FLUO-4 AM (Molecular Probes, Oregon USA), for 30–60 minutes at room temperature in the dark.

For microscopy, prepared coverslips were transferred to a PDMI-2 micro-incubator (Harvard Apparatus, Mass USA), and perfused at approx. 5 ml min$^{-1}$ (4.81–4.96 ml min$^{-1}$) with Krebs buffer at 36˚C for 5-minute wash. In some experiments the layered coverslips were then incubated for 15 minutes in 5 x $10^{-3}$ M Pyridoxalphosphate-6-azophenyl-2',4'-disulfonic acid (PPADS) and 8 x $10^{-4}$ M Adenosine 5'-triphosphate-2',3'-dialdehyde (oATP) prior to imaging without further perfusion; this was to block endogenous purinoceptors. For NOP antagonist experiments, the NOP antagonist, $10^{-6}$ M SB-612111 was added at this point. During addition of PMNs or ligands, coverslips were imaged using a Nikon Eclipse T1Si inverted confocal laser scanning microscope, using Nikon EZC1 control software, excitation via a 488nm laser, and emission recorded at 513 – 556nm using a Nikon Apochromat-plan fluor oil immersion 60x objective. Time series were recorded at 2-second intervals. Gain and laser power were determined empirically.

Extracted PMNs were incubated with 6 x $10^{-6}$ M FLUO-4 AM at 36˚C for 15 minutes, following which the cells were injected onto coverslips seeded with FLUO-4 AM loaded

CHO$_{hNOPG\alpha iq5}$. Time sequences were recorded during application of the PMNs to the prepared coverslips (drop on method-injection of 100μl Krebs buffer containing requisite number of PMN directly onto coverslip), during fMLP (as a standard PMN secretagogue [15]) stimulation and until return to baseline. Baseline fluorescence and stimulated change in relative fluorescence of PMNs and CHO cells following fMLP treatment was assessed as described below.

Image analysis was undertaken in ImageJ, inbuilt Magic Montage tool and the BioFormats plugin. Regions of interest highlighting CHO$_{hNOPG\alpha iq5}$ cells and layered PMNs were determined manually. Changes in relative fluorescence were measured as described.

### Data analysis and statistics

**Fluorimetric measurement of the change in [Ca$^{2+}$]$_i$ following ligand treatment in CHO cell populations.** for each N/OFQ concentration, the $\Delta$[Ca$^{2+}$] was calculated by subtracting the mean of 3 baseline calcium concentrations from the maximal calcium concentration following the addition of the ligand. Log[Ligand]-[$\Delta$Ca$^{2+}$]$_i$ curve fitting was performed in GraphPad Prism V9 (22 October 2020). Experiments were performed in duplicate and repeated on ≥3 sets of cells from different passages. Normality was assessed using the D'Agostino–Pearson omnibus test. Representative curves are presented showing $\Delta$[Ca$^{2+}$]$_i$ (e.g., **Fig 2A and 2B**). Concentration-response curves are presented as mean ± SEM (e.g., **Fig 2G and 2H**). Summary LogEC$_{50}$ data are presented as mean (CI95).
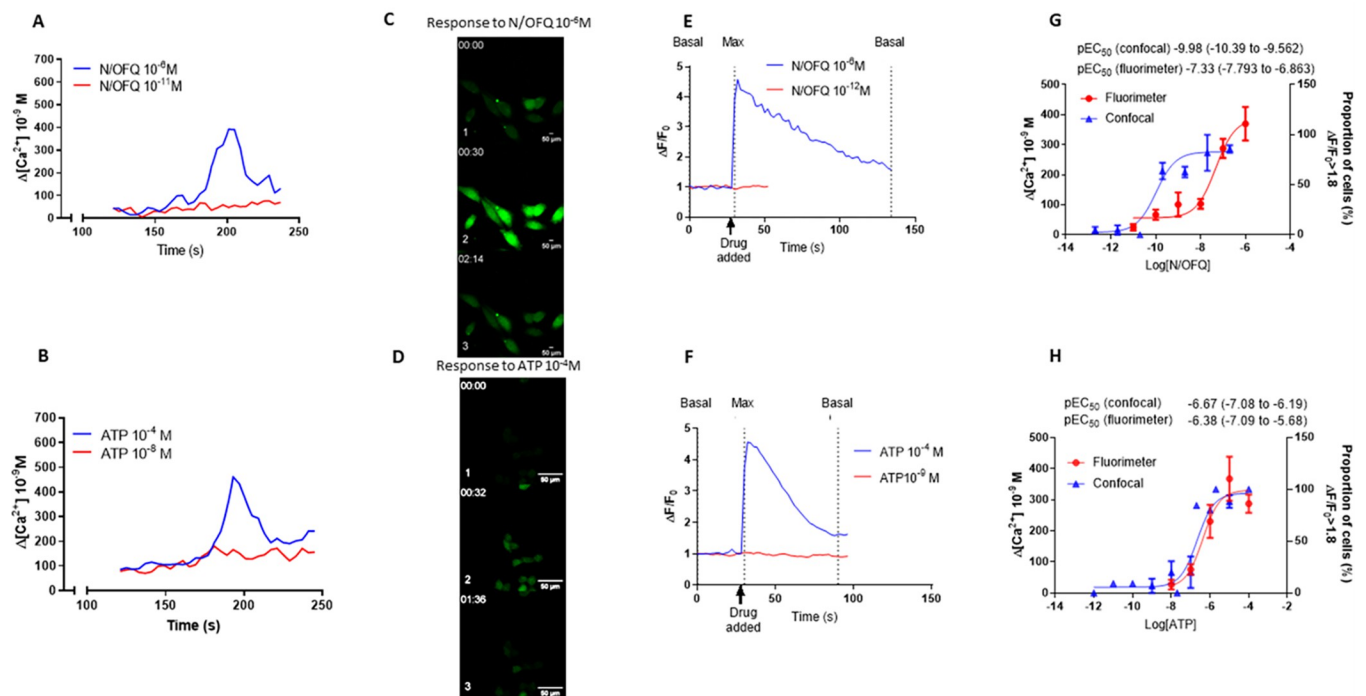


**Fig 2. Fluoroscopy and microscopy response to agonists.** A. Representative changes in intracellular [Ca$^{2+}$] in response to exposure to N/OFQ as measured by cuvette based fluorimetry using FURA-2 as an indicator dye. B. Representative changes in intracellular [Ca$^{2+}$] in response to exposure to ATP as measured by cuvette based fluorimetry using FURA-2 as an indicator dye. C. Representative change in $\Delta$F/F$_0$ in response to exposure to N/OFQ as measured by confocal microscopy using FLUO-4 as an indicator dye. (1. basal, 2. maximal, 3. decline). D. Representative change in $\Delta$F/F$_0$ in response to exposure to ATP as measured by confocal microscopy using FLUO-4 as an indicator dye (1. basal, 2. maximal, 3. decline). E. Representative change in $\Delta$F/F$_0$ in response to exposure to N/OFQ as measured by confocal microscopy using FLUO-4 as an indicator dye. F. Representative change in $\Delta$F/F$_0$ in response to exposure to ATP as measured by confocal microscopy using FLUO-4 as an indicator dye. G. Concentration-response curves showing maximal changes in intracellular [Ca$^{2+}$] as measured by fluorimetry (red; n≥3), proportion of cells where maximal $\Delta$F/F$_0$≥1.8 (blue; total 1472 cells) as measured by confocal microscopy in response to stimulation by N/OFQ. H. Concentration-response curves showing maximal changes in intracellular [Ca$^{2+}$] as measured by fluoroscopy (red; n≥3), proportion of cells where maximal$\Delta$F/F$_0$≥1.8 (blue; total 51 cells) as measured by confocal microscopy. Error bars show SEM.

**Single cell measurement of change in $[Ca^{2+}]_i$.** thresholding was used to highlight areas of increased intensity, segmented into regions of interest to represent cells. The coordinates of these defined regions of interest (ROI) are superimposed to the original image, optimised by hand, and used to measure mean fluorescent intensity within each cell. For each cell of a given cell type (for example, PMNs or CHO cells), mean fluorescence (F) was measured at 2 second intervals. $\Delta F/F_0$ was determined at each timepoint (where $\Delta F$ is $F$-$F_0$, and $F_0$ is the basal fluorescence, the mean fluorescence for the first 5 images for each region of interest). Cells with $\Delta F/F_0 > 1.8$ were classified as responsive based on a high sensitivity and low false positive rate (**see S2-S5 Figs and S1-S3 Tables in S1 File for detailed analysis methodology**). When analysing concentration-responses by confocal microscopy the $\Delta F/F_0 > 1.8$ cut-off and GraphPad Prizm were used. Statistical tests are noted in the figure legends with significance determined as $p < 0.05$.

## Results

First we needed to examine responsiveness of our biosensor $CHO_{hNOPG\alpha qi5}$ cells to (i) N/OFQ as our primary end point and the peptide we intended to assay and (ii) ATP as an identified endogenous transmitter for which CHO cells have target receptors linked to increases in $[Ca^{2+}]_i$.

Cuvette based fluorimetry demonstrates a monophasic increase in response to N/OFQ (**Fig 2A**) and ATP (**Fig 2B**). The response to N/OFQ was concentration dependent with a $pEC_{50}$ of 7.33 (95%CI 7.79–6.86) and maximal response at $10^{-6}$M (**Fig 2G**).The increase in response to ATP was also concentration dependent with a $pEC_{50}$ of 6.38 (5.68–7.09) and maximal response at $10^{-6}$ M (**Fig 2H**).

There was an increase in mean fluorescence of $CHO_{hNOPG\alpha iq5}$ cells detected by confocal fluorescence microscopy following stimulation by N/OFQ (**Fig 2C and 2E**) and this was concentration dependent, with a $pEC_{50}$ of 9.98 (9.56–10.39) and maximum at $\sim 10^{-8}$ M N/OFQ (**Fig 2G**). There was a similar increase with ATP (**Fig 2D and 2F**) yielding a $pEC_{50}$ of 6.67 (6.19–7.08) and maximum at $\sim 3 \times 10^{-6}$ M ATP (**Fig 2H**). There was a significant difference between $pEC_{50}$ for N/OFQ in cuvette and confocal systems with adherent cells in the confocal displaying a more potent response. As controls $CHO_{wt}$ cells did not respond to N/OFQ and $CHO_{hNOPG\alpha qi5}$ biosensor cells did not respond to fMLP (**S6 Fig in S1 File**).

As noted, PMNs release ATP so we next needed to confirm that we could block the effects of this transmitter in the confocal system. The response to ATP can be antagonised by the purinergic antagonists PPADS and oATP, targeted at the P2Y1, P2Y2 and P2X7 receptors. The optimal concentrations of PPADS and oATP were determined empirically (**S7 Fig in S1 File**); we elected to use $5 \times 10^{-3}$ M PPADS and $8 \times 10^{-4}$ M oATP. This combination of antagonists blocked the response of $CHO_{hNOPG\alpha qi5}$ cells to $10^{-6}$ M exogenous ATP (**Fig 3A–3C**). The proportion of responding cells (**Fig 3C**) was significantly reduced by the combined antagonists. Next we needed to know if the response to exogenously added N/OFQ could be blocked by the NOP antagonist SB-612111. In **Fig 3D–3F** the response to N/OFQ was blocked by coincubation with $10^{-7}$M SB-612111, demonstrating the antagonist ability of this ligand.

These data confirm that $CHO_{hNOPG\alpha qi5}$ is a SB-612111 sensitive detector for N/OFQ; there is also a significant response to exogenous ATP which can be antagonised by coincubation with the purinergic antagonists PPADS and oATP under the stated conditions.

Next we colayered PMNs and CHO cells. As shown in **Fig 4A and 4B**, following exposure to $10^{-6}$ M fMLP, first PMNs (identified by white arrows) and then adjacent CHO cells (identified by a yellow arrow) showed an increase in relative fluorescence, comparable to individual
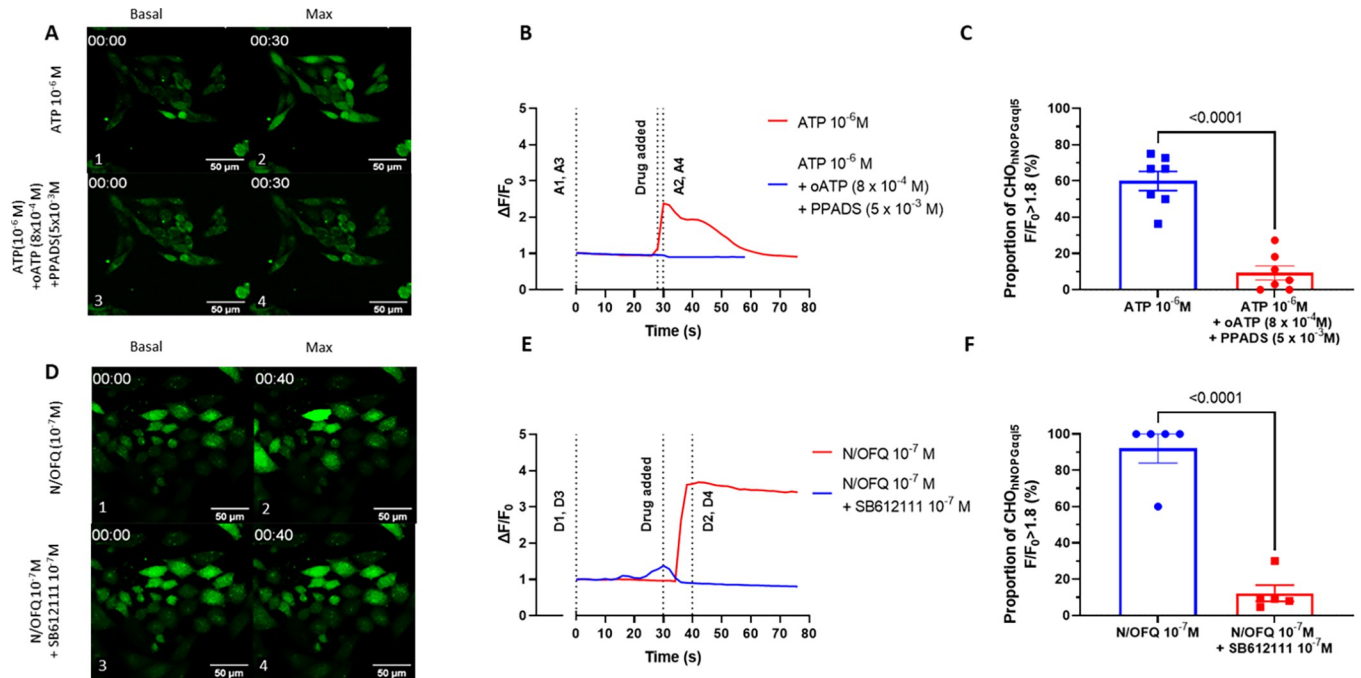
**Fig 3. Response of CHO$_{hNOPG\alpha qi5}$ to ATP and N/OFQ in the presence and absence of antagonists.** *A*. Representative change in $\Delta F/F_0$ in response to exposure to $1 \times 10^{-6}$ M ATP in the absence (1, 2), and presence (3, 4) of the purinergic antagonists PPADS $5 \times 10^{-3}$ M and oATP $8 \times 10^{-4}$ M as measured by confocal microscopy using FLUO-4 as an indicator dye. (basal 1, 3; maximal, 2, 4). *B*. Representative change in $\Delta F/F_0$ in response to exposure to $1 \times 10^{-6}$ M ATP as measured by confocal microscopy using FLUO-4 as an indicator dye in the presence and absence of PPADS and oATP in the concentrations stated. *C*. Combined cellular responses following exposure to $1 \times 10^{6}$ M ATP in the presence and absence of PPADS and oATP in the concentrations stated. *D*. Representative change in $\Delta F/F_0$ in response to exposure to $1 \times 10^{-7}$ M N/OFQ in the absence (1, 2), and presence (3, 4) of the antagonist SB-612111 $1 \times 10^{-7}$ M as measured by confocal microscopy using FLUO-4 as an indicator dye. (basal 1, 3; maximal, 2, 4). *E*. Representative change in $\Delta F/F_0$ in response to exposure to $1 \times 10^{-7}$ M N/OFQ as measured by confocal microscopy using FLUO-4 as an indicator dye in the presence and absence of $1 \times 10^{-7}$ M SB-612,111. *F*. Combined cellular responses following exposure to $1 \times 10^{-7}$ M N/OFQ in the presence and absence of $1 \times 10^{-7}$ M SB-612,111. Error bars where shown are SEM (n = 7), p values from unpaired t-test.

https://doi.org/10.1371/journal.pone.0268868.g003

responses from exposure to $10^{-6}$ M N/OFQ, suggesting an increase in intracellular calcium from NOP receptor activation. The CHO response following fMLP stimulation of colayered PMNs (**Fig 4C**) was lower than the CHO response after exposure to $10^{-6}$ M exogenous N/OFQ (**Fig 4D**). Collectively these data indicate that some of the PMNs were releasing something that is stimulating the biosensor CHO cells. Based on the above experiments with ATP we then investigaed whether there was a purinergic signal.

When coincubated PMNs (identified by white arrows) and CHO cells (identified by yellow arrows) were exposed to $10^{-6}$ M fMLP in the presence of $8 \times 10^{-4}$ M oATP and $5 \times 10^{-3}$ M PPADS, there was initiallly stimulation of PMNs followed by a delayed activation of CHO cells (**Fig 5A and 5B**). These data indicate that the response in the biosensor cells was not caused by ATP release.

Using a final protocol (with PPADS and oATP and SB-612111) of layering PMNs (identified by white arrows) onto CHO biosensor cells (identified by yellow arrows) followed by 15-minute incubation and a 10-minute wash, treatment with fMLP led to an increase in PMN but not CHO fluorescence (**Fig 6A and 6B**). Cells remained viable and responded to N/OFQ following washing of the antagonists (**Fig 6C and 6D**).

In summary, these data demonstrate a specific, repeatable increase in relative fluorescence in response to N/OFQ released from the degranulation of a proportion of the mixed PMN population. This was single cell N/OFQ release.
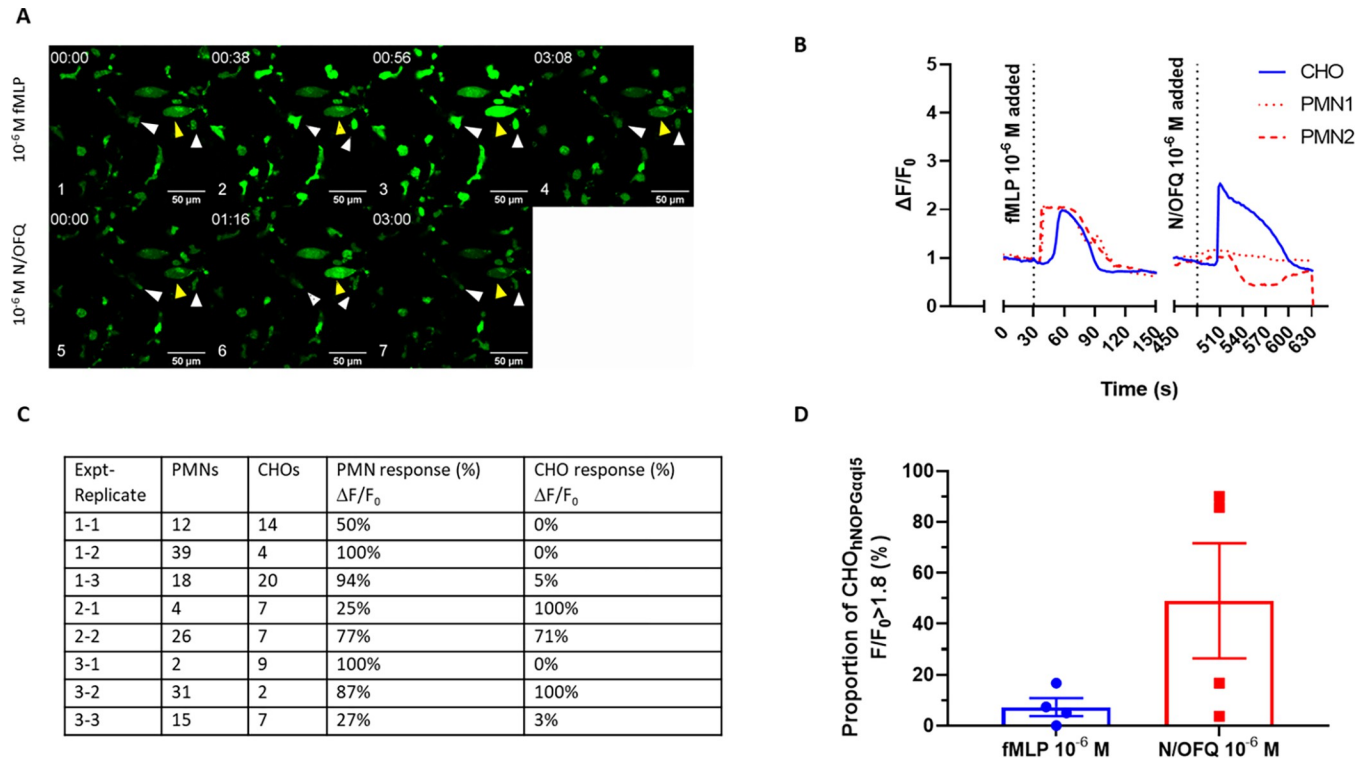
**Fig 4. Responses of CHO$_{hNOPG\alpha qi5}$ to $10^{-5}$M fMLP and $10^{-6}$M N/OFQ.** *A.* Representative change in $\Delta F/F_0$ of CHO with colayered PMNs in response to exposure to 1 x$10^{-6}$ M fMLP (1–4) and 1 x$10^{-6}$ M N/OFQ (5–8) as measured by confocal microscopy using FLUO-4 as an indicator dye. Basal 1, 5; maximal PMN, 2; maximal CHO 3, 6; return to basal, 4, 7). PMNs are identified by white arrows, while CHOhNOP$_{G\alpha qi5}$ are identified by yellow arrows. *B.* Representative single experiment showing change in $\Delta F/F_0$ of CHO cells with colayered PMNs in response to exposure to 1 x$10^{-6}$ M fMLP, washing and 1 x$10^{-6}$ M N/OFQ as measured by confocal microscopy using FLUO-4 as an indicator dye. *C.* Proportion of colayered PMN and CHO cells responsive following exposure to 1 x$10^{-6}$ M fMLP. *D.* Combined CHO cellular responses following exposure of colayered PMNs to 1 x$10^{-6}$ M fMLP, washing and then 1 x$10^{-6}$ M N/OFQ. Error bars show SEM (n = 4).

https://doi.org/10.1371/journal.pone.0268868.g004

## Discussion

The basis of this work was to identify a suitable system to detect release of N/OFQ from isolated single PMNs. Forced N/OFQ-dependent increases in $[Ca^{2+}]_i$ have been well documented in CHO$_{hNOPg\alpha i/q}$ cells using traditional fluorescence-based calcium mobilisation cuvette or microplate assays [9] and, therefore, represents the best translatable model for confocal based measurement of potential N/OFQ release.

Our initial experiments involved comparing concentration-responses for calcium increase and proportion of responsive (maximal $F/F_0 > 1.8$) cells after N/OFQ exposure in cuvette and confocal assays respectively. The estimated pEC$_{50}$ values were 7.3 and 10.0 for the cuvette and confocal assays respectively. Previous published pEC$_{50}$ values for N/OFQ in this cell line, in a microplate FLUO-4 based assay, was 9.09 [9]. There is a 500 fold difference in potency between the cuvette and confocal assay in our hands. There was also a difference between confocal and microplate potency values of around 10 fold. The lowest concentration of N/OFQ at which we were able to detect a confocal response was 100pM. It should be noted that cuvette based assays involved cells in suspension using Fura-2 while confocal assays involved measurement of adherent cells using FLUO-4. The use of different dyes is unlikely to explain the difference and we feel this is due to use of adherent cells over suspensions. In suspensions of cells using a stirred system, peptidase enzymes are more likely to be released or present in cell debris effectively metabolising and reducing N/OFQ concentrations; experiments with peptidase inhibitors
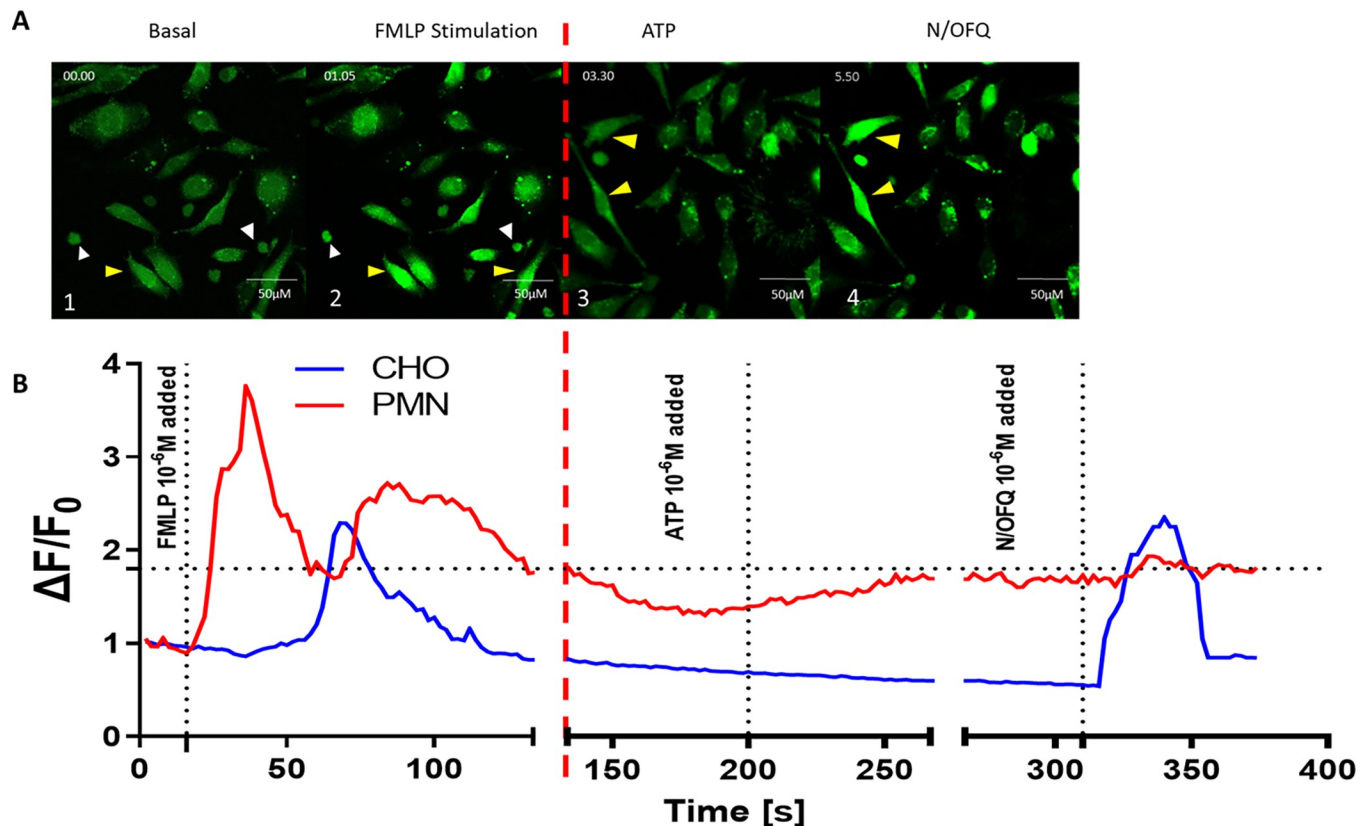
**Fig 5. CHO$_{hNOPG\alpha qi5}$ response to PMN degranulation stimulated by fMLP 1 x10$^{-6}$ M in the presence of PPADS (8 x 10$^{-4}$ M) and oATP (5 x 10$^{-3}$M).** A. Representative micrograph (from n = 6) depicting 1) basal activity, 2) fMLP stimulation of PMN and subsequent activation of CHO$_{hNOPgq/i5}$ (with representative samples of labelled CHO (yellow) and PMN (white)), 3) addition of 1x10$^{-6}$ ATP as a purinergic challenge and, finally, 4) N/OFQ to demonstrate functional viability of the CHO cells. B. Associated graph demonstrating change in $\Delta F/F_0$ following treatment with fMLP, ATP and N/OFQ. Dotted red line indicates a change of field on the same coverslip to avoid photobleaching due to the length of the experiments.

https://doi.org/10.1371/journal.pone.0268868.g005

would confirm this supposition. Comparing microplate and confocal data the latter uses a per-fusion protocol which will most likely clear the bath of enzyme activity. The lack of difference with the non-peptide ATP (below) in the two systems adds weight to our explanation. Importantly, our data indicate we can detect exogenously added N/OFQ to sub 100pM concentrations. This equates to ~181pg ml$^{-1}$. In a previous publication we summarised plasma N/OFQ concentrations in a range of assays over a range of diseases at 2.3–172 pg ml$^{-1}$. Clearly these are in total circulating volume but guide effect site ranges [16].

As noted earlier, ATP is present in PMN cells [17–19]. ATP is a damage-associated molecular pattern (DAMP) molecule, and is associated with PMN chemoattraction, phagocytosis and apoptosis. This activity in PMNs is believed to occur through ATP-sensitive, ligand-gated ion channel P2X7 receptors, with the receptor being present on lymphocytes, monocytes and macrophages [20–24]. ATP release is believed to occur when immune cells are activated [22], and as the process of cell isolation is likely to provide significant activation, ATP release is expected in these experiments. CHO cells do not express high numbers of native receptor types, making them an ideal cell line for experimentation. However, they do express two types of purinergic receptors, the P2X7 [11] and P2Y2 [10]. P2Y2 receptors are G$_q$-coupled GPCRs, whose activation also leads to increases in calcium levels. Most importantly, with regards to the development of the bioassay, activation of these purinergic receptors potentially masks any N/OFQ activity in the chimeric CHO model readout.
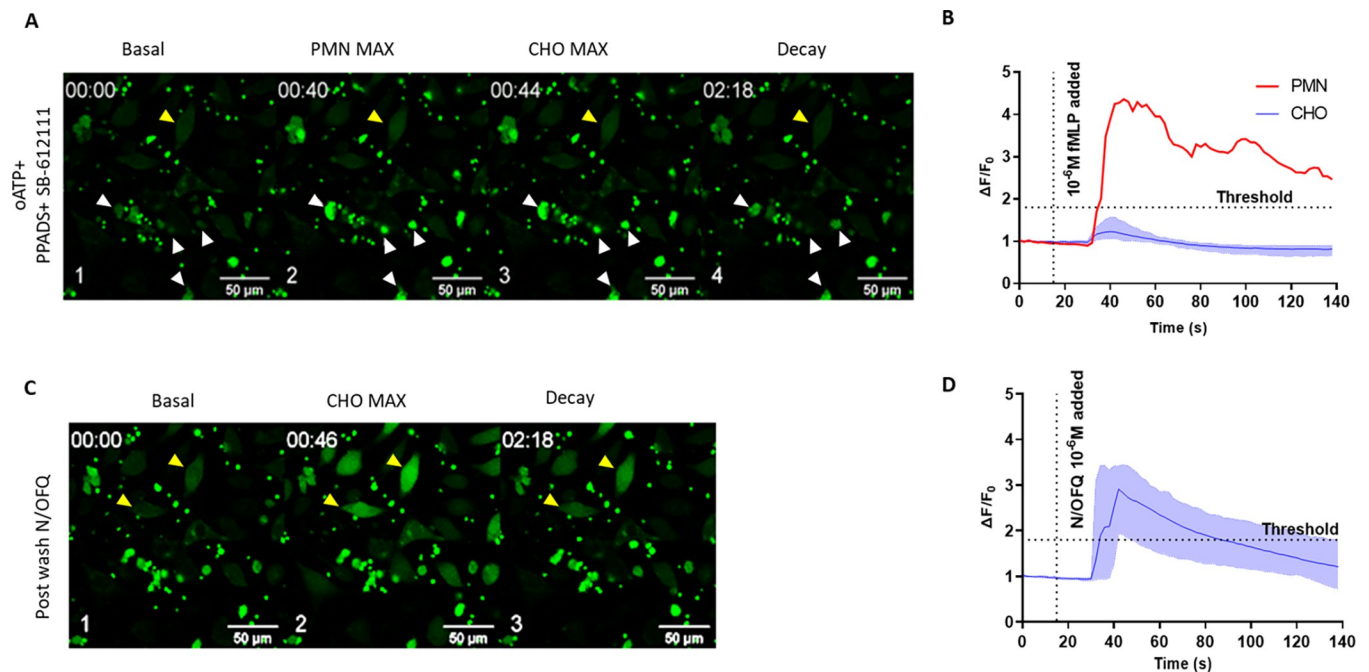
**Fig 6. CHO$_{hNOPG\alpha qi5}$ colayered with PMNs stimulated with fMLP 10$^{-6}$M in the presence of PPADS, oATP and SB-612111 do not increase calcium.** A. Representative photomicrograph (from n = 6) showing 1. Basal, 2. Maximal PMN, 3. Maximal CHO stimulation in response to 1x10$^{-6}$M fMLP in the presence of PPADS, oATP and SB-612111 measured by confocal microscopy using FLUO-4 as an indicator dye. PMNs are identified by white arrows, while CHO$_{hNOPG\alpha qi5}$ are identified by yellow arrows. B shows corresponding $\Delta F/F_0$ over time; shaded areas denote minimal and maximal response for the cell population. C. Representative photomicrograph (from n = 6) showing 1. Basal, 2. Maximal CHO stimulation in response to N/OFQ 1 x10$^{-6}$ M in the absence of antagonists. D shows corresponding $\Delta F/F_0$ over time and return of N/OFQ response; shaded areas denote minimal and maximal response for the cell population.

https://doi.org/10.1371/journal.pone.0268868.g006

CHO$_{hNOPG\alpha qi5}$ cells consequently have the machinery to respond to both N/OFQ and ATP; the former due to active transfection and the latter due to the expression of the noted endogenous purinoceptors. Effective antagonism of the purinergic signal is critical to interpretation of our data and ascription of a rise in biosensor Ca$^{2+}$ to N/OFQ and not ATP. Antgonist concentrations were chosen after a series of challenge experiments using 1x10$^{-6}$M ATP. These experiments indicated that a combination of 5x10$^{-3}$M PPADS and 8x10$^{-4}$M oATP blocked ATP-induced calcium increase (**S7 Fig in S1 File**), indicating that any remaining calcium response in the presence of these antagonists is not via purinergic signalling.

In both confocal and fluorometric experiments, ATP produced similar pEC$_{50}$ of 6.67 and 6.37 respectively. The non-peptide nature of this mediator supports our explanation above of the wide variation in N/OFQ potency in the two assay formats. Using a luciferase based assay we determined PMN ATP contents in the μM range; released contents would be lower but are likely comparable to our EC$_{50}$ values of ~0.2–0.4μM (**S8 Fig in S1 File**). Reported plasma ATP concentrations vary widely with sample preparation being an important consideration. A value of 1μM; higher around the releasing immune cells (the putative effect site) is not unreasonable [23].

In order to confirm NOP activation we have used the NOP antagonist SB-612111 [25, 26]. In our hands this antagonist has high affinity and high selectivity for NOP. In CHO cells expressing recombinant human NOP, MOP, DOP and KOP receptors SB-612111 dsiplayed K$_i$ (binding affinity) values of 0.7, >1000, >5000 and >1000 respectively. Moreover, GTPγ[$^{35}$S] binding (membranes) and cAMP (whole cells) assays at human NOP indicate antagonist K$_B$ values of 0.2 and 2.3nM respectively [25]. In the present study we used SB-612111 at the fixed concentration of 1x10$^{-7}$ to ensure selectivity of action.

We selected fMLP as our PMN 'secretagogue'. This is a simple three amino acid (n-formyl-methionyl-leucyl-phenalanine) peptide [15]. There are three formylpeptide receptors [27] and fMLP interacts with FPR1 coupled to $G_{i/o}$ and $G_z$ [28]. $G_{i\beta/\gamma}$ stimulates phospholipase-C and phosphoinositide 3-kinase to both increase $[Ca^{2+}]_i$ and activate MAPK [29, 30]. In immune cells such as PMNs this results in a wide range of actions including degranulation and chemotaxis. Indeed, degranulation is the main reason for use in this work; as an N/OFQ 'secretagogue'. In our confocal experiments we demonstrated a robust increase in $Ca^{2+}$ and this precedes activation of CHO biosensor cells.

In our initial experiments, we measured PMN stimulation with fMLP to determine whether $CHO_{hNOPG\alpha qi5}$ cells survived in the presence of these freshly isolated immune cells and whether a response to immune cell stimulation could be detected on the confocal microscope. Addition of fMLP led to an initial rise in calcium in immune cells, associated with peptide release, and following a delay, an increase in fluorescence in the CHO cells. This delayed response would indicate that substances released from immune cells has triggered a calcium response in CHO cells. In order to mitigate any potential responses produced by ATP released from immune cells the pre characterised purinergic receptor antagonist combination was added. Following fMLP stimulation, a delayed activation of $CHO_{hNOPG\alpha qi5}$ was still present, indicating the involvement of immune cell released N/OFQ. Interestingly, only some $CHO_{hNOPG\alpha qi5}$ responded following fMLP stimulation. When assessing single cell $CHO_{hNOPG\alpha qi5}$ responses when coincubated with PMNs and stimulated with fMLP, there is a clear temporal relationship between local PMN and CHO response. As this is a mixed population of PMN cells, it is possible that some but not all cells release N/OFQ following stimulation.

In a previous series of experiments we demonstrated that NOP mRNA was expressed in all immune cell populations. The presence of NOP suggests a target for feedback loops and the differential expression of N/OFQ precursor (ppN/OFQ) provides a mechanism for cell-cell interaction. With respect to the current experiments differenatial expression of ppN/OFQ and the presumed potential to release N/OFQ could explain the variability in biosensor response. Simple proximity (effect site dimensions) could also be in play.

In order to confirm whether NOP receptor activation occurs on $CHO_{hNOPG\alpha qi5}$ during this process, the NOP antagonist SB-612111 was preincubated on CHO cells with oATP and PPADS. Following addition of PMN cells and stimulation by fMLP, no activation above threshold of the $CHO_{hNOPG\alpha qi5}$ was seen, indicating that blockade of the NOP receptor has inhibited the calcium-induced increase in fluorescence. **This indicates that N/OFQ is being released from live PMN cells following stimulation**.

While it is widely accepted that N/OFQ is present within immune cells, understanding of its release is limited. In their important work studying the role of leukocytes in pain, Rittner and colleagues used flow cytometry to measure overall changes in opioid peptide expression in immune cells [31]. Following administration over several timepoints with Freuds adjuvant, a pan-opioid peptide antibody, called 3E7, detected opioid peptides amongst several immune cell subtypes. Furthermore, beta-endorphin containing cells were collected via magnetic sorting and immunohistochemistry, with the levels of beta-endorphin measured by radioimmunoassay. From these results, it was determined that in the early stages PMNs were the primary opioid-producing cells, while at later timepoints monoctyes and macrophages became the predominant opioid-containing cells. While these experiments do demonstrate that immune cells contain opioid peptides, they do not demonstrate peptide release, or what potential condition cells are in prior to opioid release. Moreover, this study focussed on classical opioids and not the N/OFQ system.

For the involvement of N/OFQ in the immune system in particular, work has either focussed on circulating N/OFQ or using non-human tissue. Previous work from our

laboratory demonstrated a significant rise in circulating N/OFQ in patients with sepsis, however the source(s) were not determined [6]. N/OFQ has been linked with arthtiritis, potentially with secretion from PMN's in the synovial fluid [8]. In this study, several experiments where undertaken to detect N/OFQ ranging from ELISA to mass spectrometry. From these results it was determined that PMN's contain N/OFQ [8]. These results compliment our findings. Our suggestion that in healthy volunteers not all PMNs secrete N/OFQ is a further refinement.

Whilst this work does demonstrate a release of N/OFQ from PMN cells our process is not without drawbacks. The most important being the process of immune cell extraction itself. This is likely to represent a major stimulus and may induce activation and degraulation thereby reducing the pool of cells capable of release. That said extracted immune cells displayed high degrees of viability and fMLP experiments showed that the vast majority of immune cells were capable of responding (as a rise in $Ca^{2+}$) to an attractant stimulus. We have been as gentle as possible in our preparatory phase and also a rapid as possible in the isolation phase. The immune cells we are using, ex vivo, from volunteers are assumed to represent the situation of PMNs in the general circulation and at rest; this may not be the case. In addition, as all immune cell types express NOP mRNA then interaction between cell types is something that could occur in vivo that we have not recreated in this bioassay.

In summary. we have designed, developed and validated a new confocal microscopy-based bioassay to detect N/OFQ release from live single immune cells. Using this assay, we have demonstrated the first evidence of live release of N/OFQ from PMNs. We plan to use this assay to explore release from individually identified immune cells (using standard immune markers) and to deploy this assay in samples from critically ill patients with sepsis.

## Supporting information

**S1 File.**
(DOCX)

## Acknowledgments

## Author Contributions

**Conceptualization:** D. G. Lambert.

**Formal analysis:** M. F. Bird, C. P. Hebbes, S. W. M. Scott, J. Willets, J. P. Thompson, D. G. Lambert.

**Funding acquisition:** J. Willets, J. P. Thompson, D. G. Lambert.

**Investigation:** M. F. Bird, C. P. Hebbes.

**Methodology:** M. F. Bird, C. P. Hebbes, S. W. M. Scott, J. Willets, D. G. Lambert.

**Project administration:** M. F. Bird, C. P. Hebbes, D. G. Lambert.

**Supervision:** D. G. Lambert.

**Writing – original draft:** M. F. Bird, C. P. Hebbes, S. W. M. Scott, J. Willets, J. P. Thompson, D. G. Lambert.

**Writing – review & editing:** M. F. Bird, C. P. Hebbes, S. W. M. Scott, J. Willets, J. P. Thompson, D. G. Lambert.

# References

1. Lambert D.G., The nociceptin/orphanin FQ receptor: a target with broad therapeutic potential. Nat Rev Drug Discov, 2008. 7(8): p. 694–710. https://doi.org/10.1038/nrd2572 PMID: 18670432

2. Toll L., et al., Nociceptin/Orphanin FQ Receptor Structure, Signaling, Ligands, Functions, and Interactions with Opioid Systems. Pharmacological Reviews, 2016. 68(2): p. 419–457. https://doi.org/10.1124/pr.114.009209 PMID: 26956246

3. Gavioli E.C., et al., Nociceptin/orphanin FQ-NOP receptor system in inflammatory and immune-mediated diseases. Vitam Horm, 2015. 97: p. 241–66. https://doi.org/10.1016/bs.vh.2014.11.003 PMID: 25677775

4. Al-Hashimi M., et al., Evidence for nociceptin/orphanin FQ (NOP) but not micro (MOP), delta (DOP) or kappa (KOP) opioid receptor mRNA in whole human blood. Br J Anaesth, 2016. 116(3): p. 423–9. https://doi.org/10.1093/bja/aev540 PMID: 26865135

5. Carvalho D., et al., The nociceptin/orphanin FQ-NOP receptor antagonist effects on an animal model of sepsis. Intensive Care Med, 2008. 34(12): p. 2284–90. https://doi.org/10.1007/s00134-008-1313-3 PMID: 18846364

6. Thompson J.P., et al., The Nociceptin/Orphanin FQ system is modulated in patients admitted to ICU with sepsis and after cardiopulmonary bypass. PLoS One, 2013. 8(10): p. e76682. https://doi.org/10.1371/journal.pone.0076682 PMID: 24124588

7. Singh S.R., et al., Nociceptin/orphanin FQ (N/OFQ) modulates immunopathology and airway hyperresponsiveness representing a novel target for the treatment of asthma. British journal of pharmacology, 2016. 173(8): p. 1286–1301. https://doi.org/10.1111/bph.13416 PMID: 26756419

8. Fiset M.E., et al., Human neutrophils as a source of nociceptin: a novel link between pain and inflammation. Biochemistry, 2003. 42(35): p. 10498–10505. https://doi.org/10.1021/bi0300635 PMID: 12950177

9. Camarda V., et al., Pharmacological profile of NOP receptors coupled with calcium signaling via the chimeric protein G alpha qi5. Naunyn Schmiedebergs Arch Pharmacol, 2009. 379(6): p. 599–607. https://doi.org/10.1007/s00210-009-0396-x PMID: 19183962

10. Iredale P.A. and Hill S.J., Increases in intracellular calcium via activation of an endogenous P2-purinoceptor in cultured CHO-K1 cells. Br J Pharmacol, 1993. 110(4): p. 1305–10. https://doi.org/10.1111/j.1476-5381.1993.tb13960.x PMID: 8306069

11. Michel A.D., et al., Identification and characterization of an endogenous P2X7 (P2Z) receptor in CHO-K1 cells. Br J Pharmacol, 1998. 125(6): p. 1194–201. https://doi.org/10.1038/sj.bjp.0702205 PMID: 9863647

12. Strober W., Trypan Blue Exclusion Test of Cell Viability. Current protocols in immunology, 2015. 111: p. A3.B.1–A3.B.3. https://doi.org/10.1002/0471142735.ima03bs111 PMID: 26529666

13. Patel A., et al., Measurement of [Ca$^{2+}$]i in whole cell suspensions using Fura-2. Methods Mol Biol, 2013. 937: p. 37–47. https://doi.org/10.1007/978-1-62703-086-1_2 PMID: 23007578

14. Grynkiewicz G., Poenie M., and Tsien R.Y., A new generation of Ca2+ indicators with greatly improved fluorescence properties. J Biol Chem, 1985. 260(6): p. 3440–50. PMID: 3838314

15. Yang K., et al., The main functions and structural modifications of tripeptide N-formyl-methionyl-leucyl-phenylalanine (fMLP) as a chemotactic factor. Die Pharmazie-An International Journal of Pharmaceutical Sciences, 2008. 63(11): p. 779–783.

16. Barnes T.A. and Lambert D.G., Editorial III: Nociceptin/orphanin FQ peptide-receptor system: are we any nearer the clinic? BJA: British Journal of Anaesthesia, 2004. 93(5): p. 626–628. https://doi.org/10.1093/bja/aeh226 PMID: 15472142

17. Bao Y., et al., Mitochondria regulate neutrophil activation by generating ATP for autocrine purinergic signaling. The Journal of biological chemistry, 2014. 289(39): p. 26794–26803. https://doi.org/10.1074/jbc.M114.572495 PMID: 25104353

18. Eltzschig H.K., et al., ATP release from activated neutrophils occurs via connexin 43 and modulates adenosine-dependent endothelial cell function. Circ Res, 2006. 99(10): p. 1100–8. https://doi.org/10.1161/01.RES.0000250174.31269.70 PMID: 17038639

19. Sueyoshi K., et al., Fluorescence imaging of ATP in neutrophils from patients with sepsis using organelle-localizable fluorescent chemosensors. Ann Intensive Care, 2016. 6(1): p. 64. https://doi.org/10.1186/s13613-016-0175-z PMID: 27422255

20. Junger W.G., Immune cell regulation by autocrine purinergic signalling. Nat Rev Immunol, 2011. 11(3): p. 201–12. https://doi.org/10.1038/nri2938 PMID: 21331080

21. Rayah A., Kanellopoulos J.M., and Di Virgilio F., P2 receptors and immunity. Microbes Infect, 2012. 14(14): p. 1254–62. https://doi.org/10.1016/j.micinf.2012.07.006 PMID: 22909902

22. Trautmann A., Extracellular ATP in the immune system: more than just a "danger signal". Sci Signal, 2009. 2(56): p. pe6. https://doi.org/10.1126/scisignal.256pe6 PMID: 19193605

23. Gorman M.W., Feigl E.O., and Buffington C.W., Human plasma ATP concentration. Clin Chem, 2007. 53(2): p. 318–25. https://doi.org/10.1373/clinchem.2006.076364 PMID: 17185366

24. Murgia M., et al., Oxidized ATP. An irreversible inhibitor of the macrophage purinergic P2Z receptor. The Journal of Biological Chemistry, 1993. 268(11): p. 8199–8203. PMID: 8463330

25. Spagnolo B., et al., Pharmacological Characterization of the Nociceptin/Orphanin FQ Receptor Antagonist SB-612111 [(–)-cis-1-Methyl-7-[[4-(2,6-dichlorophenyl)piperidin-1-yl]methyl]-6,7,8,9-tetrahydro-5H-benzocyclohepten-5-ol]: In Vitro Studies. Journal of Pharmacology and Experimental Therapeutics, 2007. 321(3): p. 961–967. https://doi.org/10.1124/jpet.106.116764 PMID: 17329552

26. Zaratin P.F., et al., Modification of Nociception and Morphine Tolerance by the Selective Opiate Receptor-Like Orphan Receptor Antagonist (–)-cis-1-Methyl-7-[[4-(2,6-dichlorophenyl)piperidin-1-yl]methyl]-6,7,8,9-tetrahydro-5H-benzocyclohepten-5-ol (SB-612111). Journal of Pharmacology and Experimental Therapeutics, 2004. 308(2): p. 454–461. https://doi.org/10.1124/jpet.103.055848 PMID: 14593080

27. He H.-Q. and Ye R.D., The Formyl Peptide Receptors: Diversity of Ligands and Mechanism for Recognition. Molecules (Basel, Switzerland), 2017. 22(3): p. 455. https://doi.org/10.3390/molecules22030455 PMID: 28335409

28. Guide to Receptors and Channels (GRAC), 4th Edition. British journal of pharmacology, 2009. 158 Suppl 1(Suppl 1): p. S1–S254.

29. Bae Y.S., et al., Activation of phospholipase C-gamma by phosphatidylinositol 3,4,5-trisphosphate. J Biol Chem, 1998. 273(8): p. 4465–9. https://doi.org/10.1074/jbc.273.8.4465 PMID: 9468499

30. Chen L.W., Lin M.W., and Hsu C.M., Different pathways leading to activation of extracellular signal-regulated kinase and p38 MAP kinase by formyl-methionyl-leucyl-phenylalanine or platelet activating factor in human neutrophils. J Biomed Sci, 2005. 12(2): p. 311–9. https://doi.org/10.1007/s11373-005-1704-1 PMID: 15917990

31. Rittner H.L., et al., Opioid peptide-expressing leukocytes: identification, recruitment, and simultaneously increasing inhibition of inflammatory pain. Anesthesiology, 2001. 95(2): p. 500–8. https://doi.org/10.1097/00000542-200108000-00036 PMID: 11506126